Multi-Range Joint Automotive Radar and Communication using Pilot-based OFDM Radar

Chang-Heng Wang[1], Onur Altintas[1], Ceyhun D. Ozkaptan[2], and Eylem Ekici[2]

[1]InfoTech Labs, Toyota Motor North America, USA
E-mail: {chang-heng.wang,onur.altintas}@toyota.com
[2]Department of Electrical and Computer Engineering, The Ohio State University, USA
E-mail: {ozkaptan.1,ekici.2}@osu.edu

2020 IEEE Vehicular Networking Conference (VNC) | 978-1-7281-9221-5/20/$31.00 ©2020 IEEE | DOI: 10.1109/VNC51378.2020.9318373

***Abstract*—To address the increasing communication demand driven by envisioned large-scale connected vehicle deployments, the dual use of the 76-81 GHz automotive radar frequency band for joint automotive radar and communication (JARC) system has gained significant interest given the wide and dedicated bandwidth. In this paper, we propose and evaluate a multi-range joint automotive radar and communication system based on pilot-based OFDM waveform. The proposed JARC system exploits the dynamic allocation of pilot subcarriers to switch between radar specifications for different ranges, e.g. short-range radar (SRR), mid-range radar (MRR) and long-range radar (LRR), to minimize the age of information of the covered regions, while dynamically adjusting the communication data rate based on traffic load.**

I. Introduction

With the upcoming large-scale deployment of Intelligent Transportation Systems (ITS), it is expected that the current allocation of 75 MHz in the 5.9 GHz spectrum would not be able to sustain every possible application and would prioritize for safety messages to improve road safety and traffic management. In order to support the wide variety of ITS applications, especially for non-safety related and high data rate ones, it is necessary to explore supplements for the 5.9 GHz spectrum. One possible and increasingly popular candidate is the dual use of radar and communication at the 76-81 GHz automotive radar band, which has several prominent advantages, including 1) a large and dedicated bandwidth is allocated for automotive radar usage, 2) efficient usage of the spectrum, and 3) reduced cost with dual use hardware and signal processing chains.

There has been extensive research on joint radar and communication in the literature, which ranges from adding data modulation on conventional radar waveforms [1], [2] to employing popular communication waveforms for radar processing [3], [4], [5]. Some examples for conventional radar waveform-based approaches include spread spectrum methods in [1] and using phase coding methods [2] on linear frequency modulated (LFM) waveform. These solutions typically compromise both communication and radar performance due to interference and the arbitrary encoding of data. For communication waveform-based approach, an IEEE 802.11ad-based radar processing is proposed in [3] to exploit the preamble of the single carrier communication frames. The radar processing approaches based on Orthogonal Frequency Division Multiplexing (OFDM) [4], [5] are attractive candidates for joint radar and communication because of the spectral efficiency, low complexity equalization, and robustness to frequency selectivity. The modulation symbol based OFDM radar processing [4] estimates the range and velocity based on the phase and frequency shifts on modulation symbols with Fourier transforms. However, the memory requirements and computational complexity for radar processing may be significant when employing large bandwidth for better radar range resolution and higher data rate. The pilot-based OFDM waveform [5] improves by focusing radar processing only on pilot subcarriers in the OFDM waveform, which enables less complexity and the possibility to use pilot sequences with perfect auto-correlation characteristics to improve radar detection quality.

Another aspect that affects the deployment cost of vehicular radar systems is the number of required radars on a vehicle. In order to satisfy the wide variety of automotive use cases, a vehicle may be required to have multiple radars with different operating ranges and field of views, even toward the same direction. For example, a vehicle may require at the front direction a long-range radar (LRR) for adaptive cruise control (ACC) and a short-range radar (SRR) for pre-crash warning. These radars typically perform detection continuously with frame rate of 20 Hz or above, however, the detection results are usually temporally correlated given the nature of road traffic. This opens up the possibility to combine multiple radars with different operating ranges into one single radar device and switch between different operating modes, e.g. [6].

In this work, we propose a multi-range joint automotive radar and communication (JARC) system, which is based on the use of the pilot-based OFDM waveform [5]. In addition to the advantage of the OFDM radar processing, the pilot-based OFDM waveform also offers the flexibility of adjusting the radar specifications, e.g. maximum unambiguous range etc., as well as the communication data rate by changing the number of allocated pilot subcarriers. We propose to dynamically adjust the pilot subcarrier allocations in the pilot-based OFDM waveform to achieve a multi-range radar and communication system with adaptive communication data rate based on the traffic load.

To formulate the scheduling problem of the multi-range

978-1-7281-9221-5/20/$31.00 ©2020 IEEE

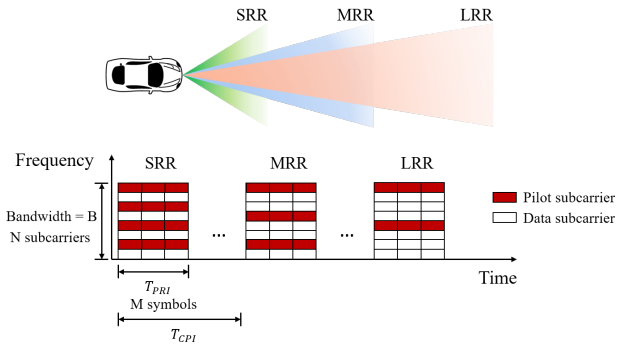

Fig. 1. Switching between different radar operation modes by dynamically adjusting pilot subcarrier allocations in Pilot-based OFDM waveform.

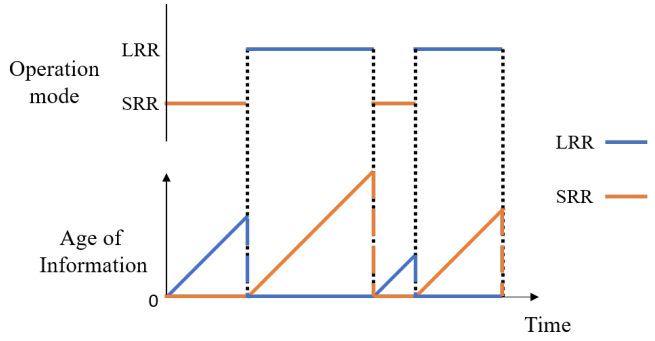

Fig. 2. The evolution of the age of information for each radar operation modes given a radar operation pattern.

radar and communication system, we introduce the *age of information* [7] performance metric in the context of radar sensing to evaluate the staleness of sensing information. In particular, for each radar operation mode, we define the age of information as the time difference between the last sensor data update time of this radar operation mode and the current time. We then pose the multi-range radar and communication scheduling as a cost minimization problem with the cost comprising the age of information of each radar operation mode and the communication traffic load.

The contributions of this work include the followings:

1) We propose the use of dynamically changing the pilot subcarrier allocation in the pilot-based OFDM waveform to achieve a multi-range joint automotive radar and communication system, and formulate the pilot subcarrier scheduling as a cost minimization problem to balance between the age of information of multi-range radar and the communication requirement.
2) We propose a greedy algorithm that minimize the instantaneous cost at any time slot, and we compare the performance of the proposed greedy algorithm with a baseline periodic pilot allocation algorithm.

II. System Model

In this section, we first briefly introduce the pilot-based OFDM waveform for JARC system and how the pilot-carrier allocation in the waveform affects the radar specification (in particular, the maximum unambiguous range) and the communication data rate. We then introduce the queueing model and the age of information, which are the two metrics we use to evaluate the multi-range JARC system.

A. Pilot-based OFDM Waveform

The bandwidth of the pilot-based OFDM waveform is denoted as B, and the total number of subcarriers is denoted as N. Among the N subcarriers, N_d subcarriers are used as data subcarriers, and N_p subcarriers are pilot subcarriers that are reserved for channel estimation and radar processing. The key radar specifications, including the range resolution Δ_R, the maximum unambiguous range $R_{\max}$, the velocity resolution Δ_v and the maximum unambiguous velocity $v_{\max}$, are given by

$$\begin{aligned} \Delta_R &= \frac{c}{2B}, R_{\max} = \frac{N_p c}{2B} \\ \Delta_v &= \frac{c}{2T_{CPI} f_c}, v_{\max} = \frac{c}{4T_{PRI} f_c} \end{aligned} \tag{1}$$

where T_{PRI} is the pulse repetition interval, and T_{CPI} is the coherent processing interval, as indicated in Figure 1.

In this work, we focus on changing the number of pilot subcarriers to adjust the maximum unambiguous range, $R_{\max}$, of the Pilot-based OFDM radar, while keeping all other specifications fixed. For the communication performance, the data rate of the joint radar and communication system depends on the number of data subcarriers allocated. Given a particular modulation and coding scheme (MCS), the effective transmitted bits for each subcarrier in a symbol is denoted as b, then the data rate is given by

$$C = \frac{N_d M b}{T_{PRI}} \tag{2}$$

In the rest of this paper, we assume that the pilot subcarrier allocation can be changed at the beginning of each coherent processing interval T_{CPI} and consider a time slotted system where the duration of each time slot is T_{CPI}.

B. Queueing Model

We assume that the data to be transmitted arrives at a single queue before it is scheduled for transmission, and the queue is operating as first-come-first-serve (FCFS). We denote the queue length at the end of time slot t as $Q(t)$. The packet arrivals at time slot t is denoted as $A(t)$, and we adopt the convention that packets arrive at the end of each time slot. Given the number of data subcarriers at time t as $N_d(t)$, the data rate according to eq.(2) would be $C(t) = \frac{N_d(t) M b}{T_{PRI}}$, and the amount of data that can be transmitted at time t is then given by $D(t) = T_{CPI} C(t)$. The evolution of the queue length can then be derived as:

$$Q(t) = \left[Q(t-1) - D(t)\right]^+ + A(t) \tag{3}$$

where $[x]^+ = \max(x, 0)$.

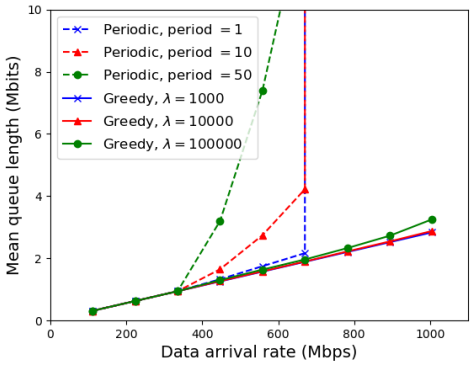

Fig. 3. Mean queue length versus data arrival rate for different scheduling policies

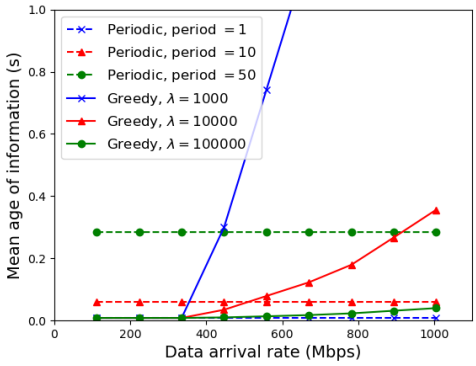

Fig. 4. Mean age of information versus data arrival rate for different scheduling policies

C. Age of Information

At any time slot t, the most recently operated time for radar operation mode m is denoted as $U_m(t)$, and we define the age of information for radar operation mode m as

$$\Delta_m(t) = t - U_m(t) \tag{4}$$

Figure 2 illustrates an example of a radar device switching between two operation modes and the corresponding evolution of the age of information for each radar operation mode. We can see that the age of information of a radar operation mode stays as zero when the radar device is currently in this operation mode, and starts accumulating once the radar switch to another operation mode.

III. Dynamic Pilot Subcarrier Allocation

In this work, we focus on the design of the scheduling policy that determines the radar operation mode at each time slot. We assume that the scheduler has access to the entire history of the system state including queue lengths and age of information as well as the past scheduling decisions.

A. Problem Formulation

In order to take both queue length and the age of information into account, we introduce a balance factor λ to combine both costs and as a parameter to adjust the trade-off between the two metrics. We then formulate the scheduling of the dynamic pilot subcarrier allocation as the following minimization problem:

$$\min \frac{1}{T}\left\{\sum_{t=0}^{T-1} Q(t) + \lambda \sum_{t=0}^{T-1}\sum_{m=1}^{M} \Delta_m(t)\right\} \tag{5}$$

B. Greedy Policy

Given the state $(Q(t-1), \Delta_1(t-1), \Delta_2(t-1), \ldots, \Delta_M(t-1))$ at the beginning of time slot t, we propose the greedy policy that determines the schedule in order to minimize the cost for time slot t. In other words, the greedy policy selects the mode $m(t)$ that minimizes the following:

$$\arg\min_{m(t)} \left\{Q(t) + \lambda \sum_{m=1} M\Delta_m(t)\right\} \tag{6}$$

Since given the state $(Q(t-1), \Delta_1(t-1), \Delta_2(t-1), \ldots, \Delta_M(t-1))$ and the scheduled radar mode $m(t)$, the queue length evolves as $Q(t) = [Q(t-1) - D_(m(t))]^+ + A(t)$, and the total age of information evolves as $\sum_{m=1}^{M} \Delta_m(t) = \sum_{m\neq m(t)} \left(\Delta_m(t-1)+1\right) = \sum_m \left(\Delta_m(t-1)\right) - \Delta_{m(t)}(t-1) + (M-1)$, we may simplify eq.(6) as maximizing the following:

$$\arg\max_{m(t)} \left\{\min\left(Q(t-1), D_m(t)\right) + \lambda\Delta_{m(t)}(t-1)\right\} \tag{7}$$

IV. Simulations

We consider three different radar operation modes, each corresponding to three different unambiguous ranges, namely short-range radar (SRR), mid-range radar (MRR), and long-range radar (LRR). The parameters of the pilot-based OFDM waveform and the corresponding radar specifications for each operation mode are listed in Table 1.

In the following paragraphs, we compare the performance between a benchmark periodic policy and the proposed greedy dynamic subcarrier allocation policy. For the benchmark periodic policy, the scheduler switches periodically between different radar operation modes (e.g. SRR, MRR, and LRR) in a round-robin fashion, using a given fixed period.

Figure 3 shows the mean queue length under different data arrival rates for each scheduling policy. Note that the maximum data rate the system can support is 1.12 Gbps, which is the maximum data rate among the three radar operation modes (SRR of 1.12 Gbps). We may first observe that the periodic policies can only support up to 745 Mbps arrival rate, which is the average data rate among three radar operation modes, above which the queue length grows unboundedly. On the other hand, the proposed greedy policy can support up to the maximum arrival rate, regardless of the value of the balance factor, and all has better delay performance compared to the periodic policy. We can also see that the queue length performance is better for smaller balance factor λ, since this implies that queue length weighs more in the cost and would favor lower queue length.

Figure 4 shows the mean age of information under different data arrival rates for each policy. Since the periodic policy

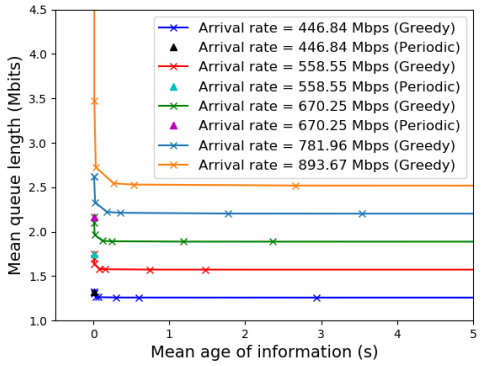

Fig. 5. Trade-off between mean queue length and mean age of information by adjusting the balance factor λ of the greedy policy under different arrival rates

switches radar operation mode in a fixed pattern, the mean age of information is a constant regardless of the data arrival rate. We also notice that the performance of the periodic policy improves monotonically when the period is shorter as in the case of mean queue length.

Figure 5 combines the two metrics and shows the trade-off between the mean queue length and the mean age of information by adjusting the balance factor λ. Each curve represents the performance trade-off between the two metrics under a fixed data arrival rate. We also show the performance of the periodic policy with period equals to 1 time slot (T_{CPI}) in the figure, which is represented as a singel data point. We can see that for each arrival rate, the data point of the periodic policy almost falls on the curve of the greedy policy, and it actually corresponds to the scenario where the mean age of information is the only metric to be minimized and the queue length performance is ignored. Note that for data arrival rates higher than 745 Mbps, the data for the periodic policy can not be shown on the figure as the queue length grows unboundedly.

In practical implementation of the system, the proper selection of the balance factor λ should depend on the targeting use case and the expected data arrival rate. For example, for general safety applications and assuming non-safety-critical communications, the balance factor should be selected to enable lower mean age of information; on the other hand, if the data traffic is supporting safety applications such as collaborative sensing, then one may consider sacrificing some freshness of the radar detection result (update rate) in exchange for benefits from collaboration with other vehicles. Regarding the dependency on the data arrival rate, if the data arrival rate is well known in advance, then the balance factor can be selected based on the desired performance tradeoff. While for the case of unknown or fluctuating arrival rate, one possible approach is to monitor the performance in real time and dynamically adjust the balance factor to strike the desired balance. Specifically, either increase the balance factor to favor lower age of information or decrease to favor queueing delay.

	Short-range radar	Mid-range radar	Long-range radar
Center frequency (f_c)	79 GHz		
Bandwidth (B)	1.0 GHz		
Number of subcarriers (N)	2048		
Symbol duration (T_{sym})	2.56 μs		
Pulse repetition interval (T_{PRI})	11.0 μs		
Coherent processing interval (T_{CPI})	2.816 ms		
Number of pilot subcarriers (N_p)	512	1024	1536
Number of data subcarriers (N_d)	1536	1024	512
Data rate (C)	1.12 Gbps	745 Mbps	372 Mbps
Range resolution (Δ_R)	0.15 m	0.15 m	0.15 m
Maximum unambiguous range ($R_{\max}$)	76.8 m	153.6 m	230.4 m

TABLE I
WAVEFORM PARAMETERS AND CORRESPONDING RADAR SPECIFICATIONS FOR DIFFERENT RADAR OPERATION MODES

V. CONCLUSIONS

In this work, we propose to dynamically adjust the pilot subcarrier locations in the pilot-based OFDM waveform to achieve a multi-range radar and communication system. We formulate a cost minimization problem to minimize a balanced cost of the communication delay and the age of information of the radar operation modes. We propose a greedy policy and compare the performance with benchmark periodic policy through simulations. For future work, we would explore the dynamic programming approach to solve for the optimal policy and compare the performance with the greedy policy. It would also be useful to consider the maximum age of information in the cost or hard constraints on age of information in the problem formulation.

REFERENCES

[1] G. N. Saddik, R. S. Singh, and E. R. Brown, "Ultra-wideband multifunctional communications/radar system," *IEEE Transactions on Microwave Theory and Techniques*, vol. 55, no. 7, pp. 1431–1437, 2007.

[2] M. J. Nowak, Zhiping Zhang, Yang Qu, D. A. Dessources, M. Wicks, and Zhiqiang Wu, "Co-designed radar-communication using linear frequency modulation waveform," in *MILCOM 2016 - 2016 IEEE Military Communications Conference*, 2016, pp. 918–923.

[3] P. Kumari, J. Choi, N. González-Prelcic, and R. W. Heath, "IEEE 802.11ad-based radar: An approach to joint vehicular communication-radar system," *IEEE Transactions on Vehicular Technology*, vol. 67, no. 4, pp. 3012–3027, 2018.

[4] C. Sturm and W. Wiesbeck, "Waveform design and signal processing aspects for fusion of wireless communications and radar sensing," *Proceedings of the IEEE*, vol. 99, no. 7, pp. 1236–1259, 2011.

[5] C. D. Ozkaptan, E. Ekici, O. Altintas, and C. Wang, "OFDM pilot-based radar for joint vehicular communication and radar systems," in *2018 IEEE Vehicular Networking Conference (VNC)*, 2018, pp. 1–8.

[6] S.-H. Jeong, H.-Y. Yu, J.-E. Lee, J.-N. Oh, and K.-H. Lee, "A multi-beam and multi-range radar with fmcw and digital beam forming for automotive applications," *Progress In Electromagnetics Research*, vol. 124, pp. 285–299, 2012.

[7] R. D. Yates, Y. Sun, D. R. B. I. au2, S. K. Kaul, E. Modiano, and S. Ulukus, "Age of information: An introduction and survey," 2020.